Self-assembled autonomous runners and tumblers

Stephen Ebbens,[1] Richard A. L. Jones,[2] Anthony J. Ryan,[3] Ramin Golestanian,[2,*] and Jonathan R. Howse[1,†]

[1]*Department of Chemical and Process Engineering, University of Sheffield, Sheffield S1 3JD, United Kingdom*
[2]*Department of Physics and Astronomy, University of Sheffield, Sheffield S3 7RH, United Kingdom*
[3]*Department of Chemistry, University of Sheffield, Sheffield S3 7HF, United Kingdom*

A class of artificial microswimmers with combined translational and rotational self-propulsion is studied experimentally. The chemically fueled microswimmers are made of doublets of Janus colloidal beads with catalytic patches that are positioned at a fixed angle relative to one another. The mean-square displacement and the mean-square angular displacement of the active doublets are analyzed in the context of a simple Langevin description, using which the physical characteristics of the microswimmers such as the spontaneous translational and rotational velocities are extracted. Our work suggests strategies for designing microswimmers that could follow prescribed cycloidal trajectories.

PACS number(s): 47.57.ef, 07.10.Cm, 87.17.Jj

For living microorganisms, their ability to direct their motion toward or away from specific targets is key to their survival. For example, in the case of *E. coli* this is achieved through temporal sensing of specific chemical signals via chemical receptors on the outer membrane of the cell that are connected with feedback loops to the motility machinery [1]. The signals would thus determine whether a cell should choose to run (i.e., move in a straight line) or tumble (i.e., randomly rotate in a same neighborhood). In the quest for making smart artificial swimming devices at the micro- and nanoscale [2], it would be ideal if such elaborate behaviors can be incorporated in the designs.

Recently several forms of such microswimmers have been made and shown to achieve autonomous motion by catalyzing reactions on an asymmetric surface [3]. These devices have been designed to produce enhanced translational displacements, and achieve this within the constraints imposed by their micron and nanoscale dimensions, which result in the eventual Brownian randomization of orientation and thus direction of propulsion direction. Examples include bimetallic nanorods [4,5] and spherical Janus particles [6]. Incorporating additional asymmetry into such swimming devices is expected to produce driven rotations or a combination of rotation and translation. This has been demonstrated in experiments where the asymmetry causing rotation has been unintentional; for example, nanorods have been reported to undergo rotation and circling due to surface pining and structural heterogeneity [5] and inhomogenous catalyst-coated spheres have been observed to perform persistent rotary motion [7]. A sophisticated dynamic shadow method has also been used to manufacture nanorotors by patterning catalyst onto silicon rods [8]. However, these devices only represent a limited sample of the wide range of trajectories that are potentially accessible by varying the relative proportions of translational and rotational propulsion, and it will be desirable to be able to make such microswimmers in a controlled way. This will open up exciting possibilities given the poten-

tial to use such swimmers as components in nanodevices, and probe physical phenomena such as the proposed inversion of the direction of confined circling microswimmers [9].

Here we report on a class of agglomerate swimmers formed by the spontaneous self-assembly of individual propulsive catalytic Janus particles that demonstrate the rich variety of trajectories achievable for swimmers with translational and angular propulsion, such as fast linear translation, spiralling, and stationary spinning motion. The experimental trajectories show a good agreement with a simple analytical model for the stochastic motion of swimmers undergoing controlled rotational and translational propulsion while subject to Brownian randomization. We analyze both positional and angular mean-square displacements within the theoretical model and extract the corresponding velocities and diffusion coefficients.

Individual platinum Janus particles were prepared by evaporating a 5 nm Platinum (Agar scientific) film onto the surface of a clean glass slide that is covered with a monolayer of polystyrene beads (2 μm diameter, Duke Scientific). The resulting asymmetric particles were transferred from the slide into 20% w/v H_2O_2 solution. After storage for several days the solution was diluted to 10% w/v H_2O_2 and transferred to a sealed cuvette (1 mm path length) for examination using a Nikon Eclipse ME600 microscope with episcopic illumination. Doublets, and larger agglomerates had formed and were observed to execute a variety of spiralling trajectories in free solution. The aggregates were allowed to settle on the bottom of the cuvette where their two-dimensional (2D) motion was recorded using a Pixelink PL-742 machine video camera and personal computer. The resulting movies were analyzed using custom image analysis software (LABVIEW) to extract positional coordinates x and y as well as orientational coordinate θ as functions of time. Videos were recorded for up to 1 h at frame rates of 3–15 fps.

Typical trajectories observed for aggregates containing two Janus particles, referred to as "doublets" henceforth, free to move in peroxide fuel and pure water are shown in Fig. 1 [10]. The addition of fuel to these doublets produced propulsion (via self-diffusiophoresis [11] as demonstrated in Ref. [6]) with a variety of trajectories ranging from linear trans-

———————
*r.golestanian@sheffield.ac.uk
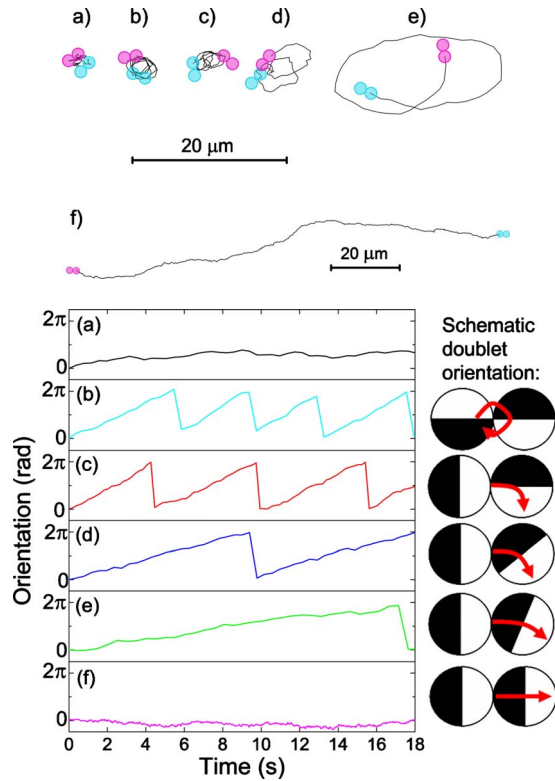†j.r.howse@sheffield.ac.uk

FIG. 1. (Color online) (Top) 25 s trajectories for a range of Janus doublets in solution: (a) Janus doublet in pure water (b-f) Janus doublets in 10% H_2O_2 with mean instantaneous velocity (v) and average angular velocity (ω) shown in Table I [pink (dark gray) and turquoise (light gray) to scale doublets show the starting and finishing position, respectively]. (Bottom) Orientation versus time plots for the trajectories shown above, and example Janus particle doublet schematic configurations corresponding to each type motion.

average angular velocities (ω) for different swimmers ranging from $0-1.3$ rad s^{-1} (see Table I). These velocities are obtained by analyzing the mean-square displacement (MSD) and the mean-square angular displacement (MSAD) within a simple Langevin description (see below). As one would expect, translational and rotational propulsions have competing effects on the trajectory of a swimmer: increased v tends to straighten up the trajectory while increased ω tends to enclose it. Observation of a large number of trajectories for different swimmers suggests that the characteristic features and repetitive patterns that swimmers exhibit are roughly identical if both v and ω are scaled by the same factor, as if their effects cancel each other (see below). The variety of v and ω observed in the experiment can be explained by considering the various possible relative orientations of the catalytic patches of the Janus particles forming the fixed doublets, shown in Fig. 1. This scheme is similar to that demonstrated on a much larger scale by the pioneering work of Whitesides *et al.*, where asymmetrically catalyst-patterned plates spontaneously formed stable doublets [12].

To quantitatively analyze the trajectories, the MSD (ΔL^2) as a function of time interval (t) is determined and shown in Fig. 2. The main distinctive feature of the MSD plots of these agglomerate swimmers as compared to simple self-propelled Janus particles [6] is a new oscillatory feature that is superimposed on the crossover behavior from propulsive to diffusive regimes. Figure 2 (left) shows the MSD plots for the trajectories in Fig. 1, which range from simple diffusive behavior to oscillatory and propulsive behaviors. The quantitative effect of angular propulsion on the MSD plots can be seen in Fig. 2 (middle), where increasing ω at (nearly) constant v is found to decrease the magnitude of MSD as well as the amplitude and period of oscillations. On the other hand, Fig. 2 (right) shows that increasing v at (nearly) constant ω increases both the magnitude of MSD and the amplitude of its oscillations.

To understand the observed behavior of tumbling swimmers, we can model their stochastic motion using a Langevin description. A detailed analysis of the dynamics of the doublets needs to take into account the anisotropy in the diffusion [13] as well as the fact that the spontaneous translational velocity (caused by propulsion) is not necessarily along one of the symmetry axes of the swimmers. For simplicity, we ignore this complexity at this stage and treat the swimmers as isotropic objects. Moreover, we treat the system as if it is intrinsically two dimensional, rather than looking at the 2D

lation through spiralling to tight rotation. This suggests that the swimmers are generating both translational and rotational propulsion. Instantaneous translational velocities (v) extracted from the distribution of successive displacements appear constant for a given trajectory, while average values vary between swimmers ($1.3-6.0$ μm s^{-1}) as presented in Table I. Persistent angular propulsion is also present for all but the control (trajectory a) and linearly translating (trajectory f) swimmers, as shown in Fig. 1. Here, the rotation rate appears to be an intrinsic property of a given doublet, with

TABLE I. Extracted physical parameters for the tumbling swimmers whose trajectories are shown in Fig. 1, from fitting the experimental data to Eqs. (4) and (5).

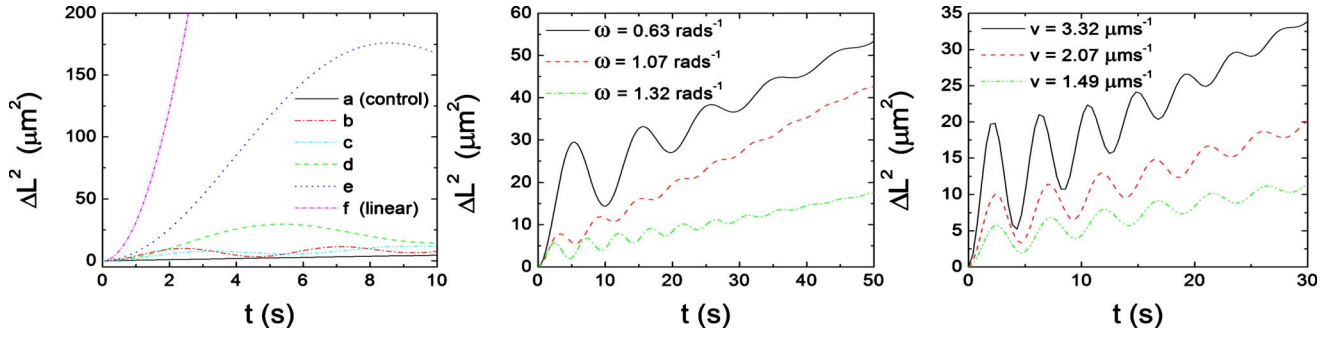| Trajectory	ω (rad s^{-1}) from MSAD	τ_r (s) from MSAD	τ_r (s) from MSD	D (μm^2 s^{-1}) from MSD	v (μm s^{-1}) from MSD	ω (rad s^{-1}) from MSD
a	0	14.5	n/a	0.10	0	0
b	1.32	11.1	19.2	0.06	2.07	1.35
c	1.08	16.4	15.6	0.15	1.30	1.07
d	0.63	22.7	21.3	0.07	1.66	0.63
e	0.39	20.5	24.5	0.03	2.80	0.49
f	0	21.8	14.1	0.09	5.99	0

FIG. 2. (Color online) (Left) Mean-square displacements versus time for selected trajectories shown in Fig. 1. (Middle) Effect of ω on MSD plots (from top to bottom $v = 1.65$, 1.30, and 1.49 μm s^{-1}, respectively). (Right) Effect of v on MSD plots (from top to bottom $\omega = 1.49$, 1.35, and 1.32 rad s^{-1}, respectively).

projection of a three-dimensional (3D) motion as done in Ref. [6]. This assumption is supported by the experimental observation that the doublets tend to stay near the substrate once settled there, and exhibit 2D motion parallel to the surface. The Langevin equations for the position $\mathbf{r}(t) = (x(t), y(t))$ and orientation $\theta(t)$ of the swimmer can be written as

$$dx(t)/dt = v \cos \theta(t) + \xi_1(t), \tag{1}$$

$$dy(t)/dt = v \sin \theta(t) + \xi_2(t), \tag{2}$$

$$d\theta(t)/dt = \omega + \zeta(t), \tag{3}$$

where the noise terms ξ_i and ζ are Gaussian random variables with zero mean, and their correlators read $\langle \xi_i(t) \xi_j(t') \rangle = 2D \delta_{ij} \delta(t-t')$, $\langle \zeta(t) \zeta(t') \rangle = 2D_r \delta(t-t')$, and $\langle \xi_i(t) \zeta(t') \rangle = 0$ (for $i,j = 1,2$). Here, D is the translational diffusion coefficient of the swimmer (that is assumed to be isotropic for simplicity) and D_r is the rotational diffusion coefficient, from which the rotational diffusion time can be defined via $\tau_r = 1/D_r$. Equation (3) is decoupled from the others and can be integrated on its own to yield

$$\Delta\theta^2(t) \equiv \langle [\theta(t) - \theta(0)]^2 \rangle = \omega^2 t^2 + 2D_r t, \tag{4}$$

for the MSAD. We can also calculate the velocity ($\mathbf{v}(t) = d\mathbf{r}(t)/dt$) auto-correlation function, which reads $\langle \mathbf{v}(t) \cdot \mathbf{v}(0) \rangle = 4D \delta(t) + v^2 \cos \omega t e^{-D_r t}$. The MSD can then be calculated as $\Delta L^2(t) \equiv \langle [\mathbf{r}(t) - \mathbf{r}(0)]^2 \rangle = \int_0^t dt_1 \int_0^t dt_2 \langle \mathbf{v}(t_1) \cdot \mathbf{v}(t_2) \rangle$. We find

$$\Delta L^2(t) = 4Dt + \frac{2v^2 D_r t}{D_r^2 + \omega^2} + \frac{2v^2(\omega^2 - D_r^2)}{(D_r^2 + \omega^2)^2}$$

$$+ \frac{2v^2 e^{-D_r t}}{(D_r^2 + \omega^2)^2}[(D_r^2 - \omega^2)\cos \omega t - 2\omega D_r \sin \omega t]. \tag{5}$$

The above result shows that the MSD starts off as $4Dt + v^2 t^2$ for $t \ll \tau_r \& 1/\omega$ like a simple self-propelled particle, goes through an oscillatory period for $1/\omega < t < \tau_r$ (provided $1/\omega < \tau_r$) and crosses over to a purely diffusive regime with the effective diffusion coefficient

$$D_{\text{eff}} = D + \frac{v^2 \tau_r}{2[1 + (\omega\tau_r)^2]}. \tag{6}$$

This shows that in the limit where $\omega\tau_r \gg 1$, the effective diffusion coefficient that determines the long-time behavior of the swimmers is only a function of v/ω, which means that scaling both v and ω by the same factor does not produce a different type of motion, as observed in our experiments. In the opposite limit where $1/\omega > \tau_r$, the crossover from propulsive to diffusive behavior precludes the appearance of the oscillatory regime. The physical origin of this crossover effect (that causes dampening of the oscillations seen in the MSD vs time plots for rotationally propulsive swimmers) is the cumulative effect of Brownian rotation which reduces the correlation between the orientation of the swimmer as a function of time.

The experimental trajectories were analyzed within the above simple analytical description, by fitting the MSD and MSAD data to Eqs. (4) and (5). All cases showed a near collapse of the experimental data on the analytical fits in the relevant time domain, as the example of Fig. 3 shows. All fits were performed for the first 10 s of the plots, except for the non-rotating case (trajectory f) where the fit was performed for the first 1 s because the fast linearly propelling microswimmer would leave the field of view very quickly. Us-
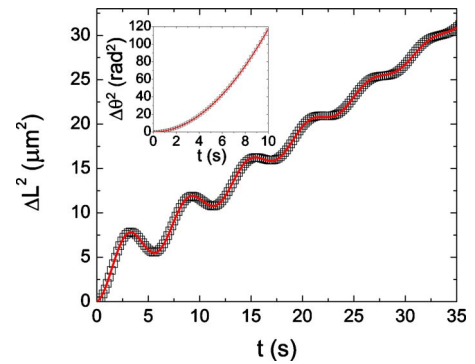

FIG. 3. (Color online) Example unconstrained fit to 10 s of Janus doublet MSD data corresponding to trajectory c in Fig. 1. The fit yields $D = 0.15$ μm^2 s^{-1}, $\tau_r = 15.6$ s, $v = 1.30$ μm s^{-1}, and $\omega = 1.07$ rad s^{-1}. Inset: Quadratic fit to mean-square angular data, yielding $\omega = 1.08$ rad s^{-1} and $\tau_r = 16.4$ s.

ing the fits we could extract the values of v, ω, D, and τ_r, as reported in Table I. It is important to note that using the above model—that corresponds to spherical particles—to analyze the trajectories of doublets introduces a systematic error, which will affect the estimates for D and τ_r.

The two parameters ω and τ_r can be determined independently from both the MSD and MSAD fits, and comparing these estimates provides a consistency check. We find (see Table I) that the independent estimates are in very good agreement for ω, which should be less affected by the anisotropy effect. The two fitted estimates of the rotation time τ_r are in reasonable agreement, mainly differing by a systematic error and showing no strong dependency on v and ω. We find an average of $\tau_r = 18 \pm 3$ s from the MSAD fits and $\tau_r = 20 \pm 2$ s from the MSD fits. The translational diffusion coefficient is fitted less accurately, yielding an average value of $D = 0.08 \pm 0.03$ μm^2 s^{-1}. This is presumably due to the effect of anisotropy mentioned above, as well as the fact that there is insufficient information about the translational behavior of the swimmer in the experimentally accessible initial part of the MSD curve, where propulsion dominates. For comparison, we can make estimates of these intrinsic parameters using the analytical expressions $D^{\text{sphere}} = k_B T / (6 \pi \eta R)$ and $\tau_r^{\text{sphere}} = 8 \pi \eta R^3 / k_B T$ for a sphere of radius R, where $k_B T$ is the thermal energy and η is the viscosity of water. Using $\eta = 10^{-3}$ Pas, $T = 22$ °C, and a nominal radius $R = 2$ μm (equal to the diameter of our colloidal beads), we find $D^{\text{sphere}} = 0.1$ μm^2 s^{-1} and $\tau_r^{\text{sphere}} = 22$ s, which is in reasonable agreement with the above values.

Finally, we note that the self-assembly leading to the formation of the doublets appeared to produce a random distribution of relative particle orientations, with no bias toward any particular configuration despite the heterogeneous nature of the individual swimmer surface. In our experiments, most doublets formed by self-assembly would rotate, and linear translators were rare (out of the >100 doublets observed only one linear translator was seen, along with one perpendicular translator), which is consistent with the low probability of this alignment occurring. In addition to the doublets discussed here, higher order aggregates of up to six beads, in a variety of morphologies were also observed to undergo persistent motion. The motion of these larger objects could also be described within the model presented above.

In summary, we have demonstrated the self-assembly of individually propulsive Janus particles into autonomous swimmers with a wide variety of trajectories and morphologies. The experimental findings have been accounted for reasonably well by a simple Langevin description that ignores the anisotropy of the doublet. It is hoped that the class of microswimmers will make possible investigations into the many-body behavior of spiraling low-Reynolds number swimmers, and find use as easy-to-make small scale transporters and assemblers with a wide range of paths.

[1] H. C. Berg, *E. coli in Motion* (Springer-Verlag, New York, 2004).

[2] W. F. Paxton *et al.*, Angew. Chem., Int. Ed. **45**, 5420 (2006) and references therein.

[3] For a recent review, see S. J. Ebbens and J. R. Howse, Soft Matter **6**, 726 (2010).

[4] W. F. Paxton *et al.*, J. Am. Chem. Soc. **126**, 13424 (2004); D. Kagan *et al.*, *ibid.* **131**, 12082 (2009).

[5] S. Fournier-Bidoz *et al.*, Chem. Commun. (Cambridge) **2005**, 441.

[6] J. R. Howse *et al.*, Phys. Rev. Lett. **99**, 048102 (2007).

[7] J. Vicario *et al.*, Chem. Commun. (Cambridge) **2005**, 3936.

[8] Y. He, J. Wu, and Y. Zhao, Nano Lett. **7**, 1369 (2007).

[9] S. van Teeffelen, U. Zimmermann, and H. Löwen, Soft Matter **5**, 4510 (2009).

[10] See supplementary material at http://link.aps.org/supplemental/10.1103/PhysRevE.82.015304 for movies showing the trajectories of the tumbling microswimmers.

[11] R. Golestanian, T. B. Liverpool, and A. Ajdari, Phys. Rev. Lett. **94**, 220801 (2005); New J. Phys. **9**, 126 (2007).

[12] R. F. Ismagilov *et al.*, Angew. Chem., Int. Ed. **41**, 652 (2002).

[13] F. Perrin, J. Phys. Radium **5**, 497 (1934); **7**, 1 (1936); Y. Han *et al.*, Science **314**, 626 (2006); C. Ribrault, A. Triller, and K. Sekimoto, Phys. Rev. E **75**, 021112 (2007).